Chinese Journal of Physiology 55(6): 380-389, 2012
DOI: 10.4077/CJP.2012.BAA047

A Requirement of Low-Threshold Calcium Spike for Induction of Spike-Timing-Dependent Plasticity at Corticothalamic Synapses on Relay Neurons in the Ventrobasal Nucleus of Rat Thalamus

Ching-Lung Hsu[1, †], Hsiu-Wen Yang[3, 4], Cheng-Tung Yen[1], and Ming-Yuan Min[1, 2]

[1]*Institute of Zoology and* [2]*Department of Life Science, College of Life Science, National Taiwan University, Taipei 10617*
and
[3]*Department of Biomedical Sciences and* [4]*Department of Medical Research, Chung-Shan Medical University, Taichung 40201, Taiwan, Republic of China*

Abstract

Relay neurons in sensory thalamus transmit somatosensory information to cerebral cortex and receive sensory and feedback corticothalamic (CT) synaptic inputs. Their duality of firing modes, in bursts and continuous, underlies state dependence of thalamic information transfer, but the impact of different firing patterns on synaptic plasticity was rarely explored. To address this issue, we made whole-cell recording from relay neurons in the ventrobasal nucleus (VBN) of rat thalamus and compared synaptic plasticity induced by pairing CT-EPSP with two different types of burst spiking: low-threshold spike (LTS)-burst spiking triggered at V_m~-70 mV, and high-frequency spiking induced at V_m~-55 mV. The latter mimics natural burst spiking of relay neurons without activation of LTS. We found that, while backpropagating APs alone were not sufficient, low-threshold calcium spike was required for the induction of spike-timing-dependent LTP at CT synapses. Our results reveal a novel role of the calcium spike plays in the induction of long-term plasticity of CT synapse. Considering the dendritic origin of LTS, this study also implies potential physiological regulations over synaptic plasticity in thalamus. We propose that this form of synaptic plasticity may be involved in the dynamic fine-tuning of thalamocortical information relay.

Key Words: corticothalamic (CT) synapse, long-term potentiation (LTP), low-threshold calcium spike, somatosensory, ventrobasal nucleus (VBN)

Introduction

The ventrobasal nucleus (VBN) of thalamus serves as a major gateway for relaying sensory information from periphery to cerebral cortex (11). VBN relay neurons receive primary sensory inputs from medial lemniscus (*ml*) and corticothalamic (CT) feedback inputs from higher cortical areas (11, 17,

Corresponding authors: [1] Ching-Lung Hsu, Ph.D., Institute of Zoology, National Taiwan University, No. 1, Sec. 4, Roosevelt Rd., Taipei 10617, Taiwan, ROC. Tel: +886-2-33664535, Fax: +886-2-23673374, E-mail: b90205125@ntu.edu.tw; and [2] Ming-Yuan Min, Ph.D., Institute of Zoology, National Taiwan University, No. 1, Sec. 4, Roosevelt Rd., Taipei 10617, Taiwan, ROC. Tel: +886-2-33664535, Fax: +886-2-23673374, E-mail: mymin@ntu.edu.tw
[†]Current address: Janelia Farm Research Campus, Howard Hughes Medical Institute, 19700 Helix Drive, Ashburn, VA 20147, USA. (e-mail: hsuc@janelia.hhmi.org)
Received: June 16, 2011; Revised: December 12, 2011; Accepted: December 29, 2011.
 ISSN : 0304-4920. http://www.cps.org.tw

31). There are two types of CT fibers, arising from cortical layer V and VI pyramidal neurons, respectively, with the latter dominating the number of CT projections to somatosensory thalamus in rodents (3, 12, 26, 27, 33). Considering the predominance in the number of synaptic contacts onto thalamic relay neurons, CT input was regarded as an essential modulator for the properties of thalamic spike transfer (4, 6, 11, 13, 24, 30).

Many efforts have been made to elucidate the neuronal basis for information processing and transfer operated within the thalamus, particularly on the intrinsic firing properties of thalamic relay neurons (1, 5, 10, 11, 13, 16, 20, 22, 28, 29, 36). At hyperpolarized membrane potential, low-threshold spike (LTS) is initiated by T-type voltage-gated calcium channels (T-VGCCs), which drives high-frequency burst spiking (10, 11, 29, 36) and is proposed to underlie the state dependence of thalamic relay (11, 16, 20, 28, 29).

Given that synaptic drive from CT feedback can play critical roles in switching of firing mode and modulation of thalamocortical functions (4, 6, 11, 13, 24, 30, 35), use-dependent change in the efficacy of CT input could be a mechanism underlying dynamic information processing and relay in thalamus. In a recent study, we systematically analyzed the fast excitatory synaptic transmissions from cortex and *ml* onto the VBN relay neurons of rat thalamus, and demonstrated such a flexibility of CT feedback strength (9). We reported the differential expression of ionotropic glutamate receptor content, N-methyl-D-aspartate receptor (NMDAR)-dependent long-term potentiation (LTP) and L-type voltage-gated calcium channel (L-VGCC)-dependent long-term depression (LTD) between sensory and cortical inputs on thalamic relay neurons in the VBN. Furthermore, we found that L-VGCC-dependent LTD of CT synaptic transmission could be induced only with a specific type, namely the continuous, firing mode. These findings provide a plausible neuronal basis on which CT synapses may act as a detector for recent activities of thalamic relay, and the corresponding modification of CT synaptic input can exert a feedback influence on the thalamic information transfer. In this study, we investigated whether CT synaptic input expresses spike-timing-dependent LTP, a more physiologically relevant form of Hebbian plasticity (2), and whether its induction also depends on a specific firing mode of thalamic relay neurons in the VBN.

Materials and Methods

Preparation of Thalamic Slices

The use of animals in this study was in accordance with guidelines of the Ethical Committee for Animal Research of National Taiwan University. Sprague-Dawley rats aged 13~24 days were used. The rats were decapitated, and their brains were quickly removed and placed in ice-cold artificial cerebrospinal fluid (ACSF), consisting of (in mM): 119 NaCl, 2.5 KCl, 1.3 $MgSO_4$, 26.2 $NaHCO_3$, 1 NaH_2PO_4, 2.5 $CaCl_2$, and 11 glucose; the pH was adjusted to 7.4 by gassing with 95% O_2 and 5% CO_2. Coronal or horizontal slices of 300-μm thickness containing the VBN and internal capsule (*ic*; Fig. 1A) were cut using a vibroslicer (ZERO 1, D.S.K., Osaka, Japan). The slices were kept in oxygenated ACSF (95% O_2 and 5% CO_2) at room temperature (24~25°C) for 60~90 min to allow recovery before recording commenced.

Electrophysiology

Slices were transferred to an immersion-type recording chamber mounted to an upright microscope (BX50WI, Olympus Optical, Tokyo, Japan) equipped with an infrared-differential interference contrast microscopic video. The VBN and *ic* were clearly identified under low magnification (Fig. 1A). Neurons in the VBN were recorded under visual guidance with patch pipettes pulled from borosilicate glass (1.5-mm outer diameter, 0.32-mm wall thickness; G150F-4, Warner Instruments, Hamden, CT, USA). The patch electrodes had a resistance of 3~8 MΩ when filled with a solution consisting of (in mM): 131 K-gluconate, 20 KCl, 10 HEPES, 2 EGTA, 8 NaCl, 2 ATP, 0.3 GTP, and 6.7 biocytin; the pH was adjusted to 7.2 by KOH and osmolarity to 300~305 mOsm. Recordings were made with an Axopatch 1D amplifier (Molecular Devices, Union City, CA, USA) at room temperature. For current-clamp recording, input resistance (Ri) was constantly monitored by applying a current pulse of -10~-30 pA, and the bridge was balanced by adjusting the series resistance (Rs) compensation of the amplifier. Rs was typically less than 25 MΩ. Data were discarded when Ri varied by more than 20% of its value during the recording of baseline. All signals were low-pass filtered at the corner frequency of 2 kHz and then digitized at 10 kHz using a Micro 1401 interface (Cambridge Electronic Design, Cambridge, UK). Data were collected using Signal software (Cambridge Electronic Design, Cambridge, UK).

The excitatory postsynaptic potential of CT synapse (CT-EPSP) was evoked and characterized based on previously reported criteria (9, 22). Briefly, slices were constantly perfused with ACSF containing 0.1 mM picrotoxin and 1 μM strychnine to isolate pure excitatory activities. A bipolar stainless steel electrode (FHC, St. Bowdoin, ME, USA) was placed locally in the VBN or *ic* (in horizontal slices); CT-

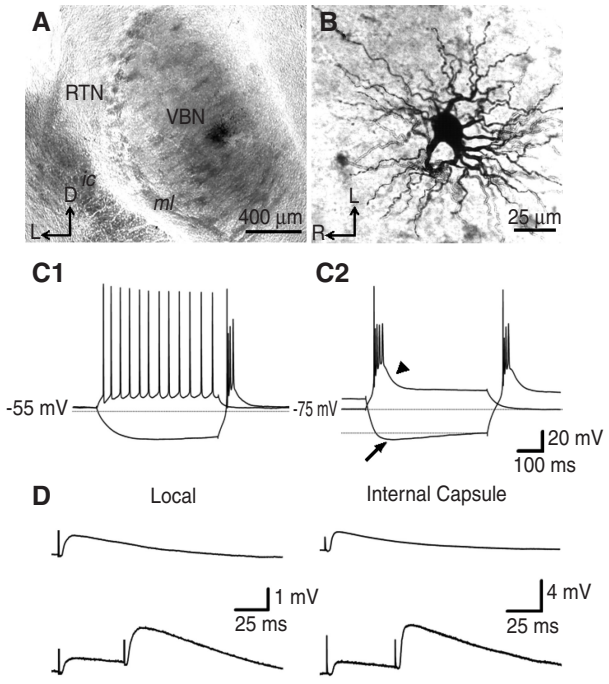

Fig. 1. Identification of the ventrobasal nucleus (VBN) and recording of corticothalamic (CT) EPSP. *A*, A photograph of a typical coronal slice used in this study. A bipolar stimulating electrode was placed in the vicinity of the recorded neurons for eliciting CT-EPSPs. The darker region in the VBN represents the recorded neurons after histochemical visualization of the injected biocytin. *ic*: internal capsule; *ml*, medial lemniscus; RTN, reticular nucleus; VBN: ventrobasal nucleus; D: dorsal; L: lateral. *B*, A biocytin-filled thalamic relay neuron located in the VBN. L: lateral; R: rostral. *C*, Voltage responses of a VBN relay neuron upon current injections. A depolarizing current pulse induced continuous spiking with the V_m held at ~-50 mV (C1, upper trace), or a low-threshold spike (LTS, arrow head) with high-frequency burst spiking with the V_m held at ~-75 mV (C2, upper trace); a hyperpolarizing current pulse induced rebound LTS-burst spiking (both lower traces). Note the voltage sag was induced at a more hyperpolarized V_m (C2, arrow). *D*, Examples of CT-EPSPs evoked by local (120 μA, 100 μs) and *ic* (40 μA, 100 μs) stimulation with single (upper traces) and paired pulses (lower traces). The traces are the responses averaged over 10 sweeps of recording. Note that they showed similar kinetics and short-term plasticity.

EPSPs were evoked by electrical stimulation (4~100 μs square pulse with the amplitude of 30~800 μA at 0.1 Hz), and no significant differences were observed between the responses evoked in these two conditions (Fig. 1D). Unless specified, the V_m of the recorded thalamocortical (TC) relay neurons was held at -70 mV. The estimated liquid junction potential was ~+10 mV and was left uncorrected. For CT-EPSP activity in the current-clamp mode, data were accepted if the EPSP had a smooth rising phase and an exponentially decaying phase in the recording of baseline; the data with signs of NMDAR-mediated activity on the decay phase of EPSPs, characterized by the appearance of a slow component (14), were discarded.

For LTP experiments, a stable baseline was recorded for at least 5 min, followed by at least 30 min of recording after pairing CT-EPSP with LTS-burst spiking or high-frequency spiking at 0.167 Hz for 100 times (Fig. 2, A2 and B2; Fig. 4, A2 and B2). CT-EPSPs were evoked at 0.1 Hz. Time interval of pairing (Δt) was defined by the average difference in time between the onset of the CT-EPSP and the peak of the 1st action potential (AP). We referred to "positive" ($\Delta t > 0$) pairing as by which the CT-EPSP onset led the 1st AP, whereas "negative" ($\Delta t < 0$) pairing as by which the CT-EPSP onset lagged the 1st AP. LTS-burst spiking was induced by one 1~2-ms or 200-ms somatic current injections with the V_m held at ~-70 mV. There was no significant difference in synaptic plasticity induced between these two conditions and the data were pooled. High-frequency spiking was induced by five 1-ms somatic current injections at 125 Hz (the average number and frequency of AP spiking of a typical LTS-burst) with the V_m held at ~-55 mV.

Drugs

The chemicals used for the ACSF and internal solution were purchased from Merck (Darmstadt, Germany). DL-APV and mibefradil were purchased from Tocris Cookson (Bristol, UK). MgATP, NaGTP, BAPTA, picrotoxin, strychnine and nickel chloride were purchased from Sigma (St. Louis, MO, USA).

Data Analysis and Statistics

For the LTP experiments, the initial slope of CT-EPSP was monitored and normalized to that of the baseline average response, and the average CT-EPSP slope recorded 25~30 min after pairing was used for statistical comparison. LTS depolarization (Fig. 3, B3) was calculated as the difference between the membrane potential before the current injection and that just after the last AP of LTS-burst spiking, which is a measure of LTS plateau and typically at ~40 ms following the 1st AP. The membrane potential following the last AP occasionally reached the threshold and evoked an additional AP; however, it was included for analysis as long as the additional AP firing did not affect the measurement. For residual depolarization following high-frequency spiking, the difference between the membrane potential before all current injections and that just after the 5th somatic

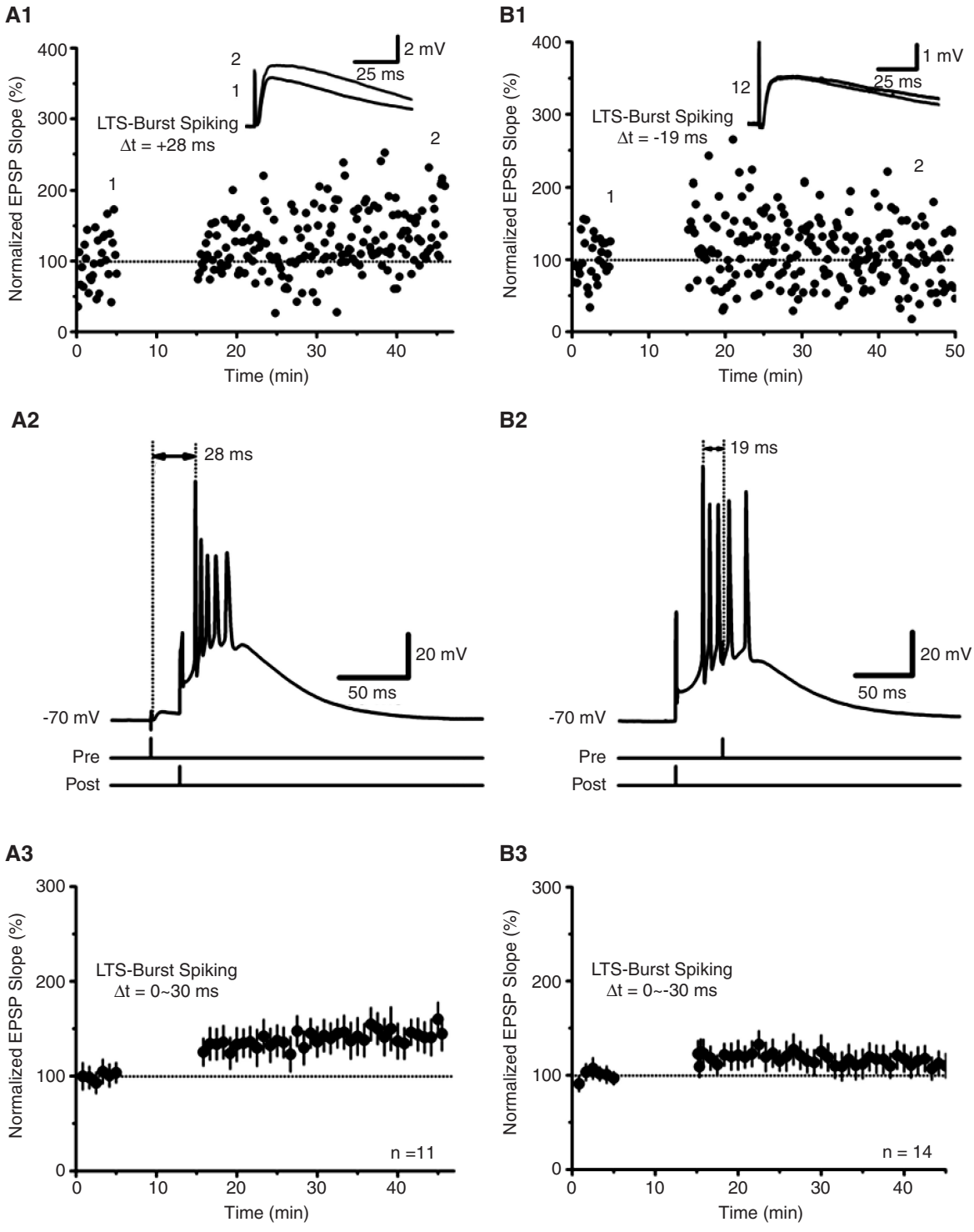

Fig. 2. Spike-timing-dependent plasticity of CT-EPSP induced by pairing CT-EPSP with LTS-burst spiking. *A*, Typical example of the time course of CT-EPSP initial slope normalized with respect to the baseline (dots in A1), representative voltage trace during the pairing (A2), and summarized time course (A3) of the experiments in which LTP was induced by pairing CT-EPSP with LTS-burst spiking at positive intervals (Δt = 0~30 ms). *B*, Typical example of the time course of normalized CT-EPSP initial slope (dots in B1), representative voltage trace during the pairing (B2), and summarized time course (B3) of the experiments in which CT-EPSP was paired with LTS-burst spiking at negative intervals (Δt = 0~-30 ms). The inset traces in A1 and B1 are the responses averaged over 10 sweeps of recording during baseline ("1") and 30 min after pairing ("2"). The line drawings at the bottom of A2 and B2 indicate the timing of extracellular stimulation ("Pre"; 530 μA, 50 μs in A2 and 238 μA, 50 μs in B2) and somatic current injection ("Post"; 1.86 nA, 2 ms in A2 and 2 nA, 1 ms in B2), which were paired at 0.167 Hz for 100 times. Note that the V_m during pairing was ~-70 mV, and a significant LTP was induced only with positive pairing (Fig. 2A).

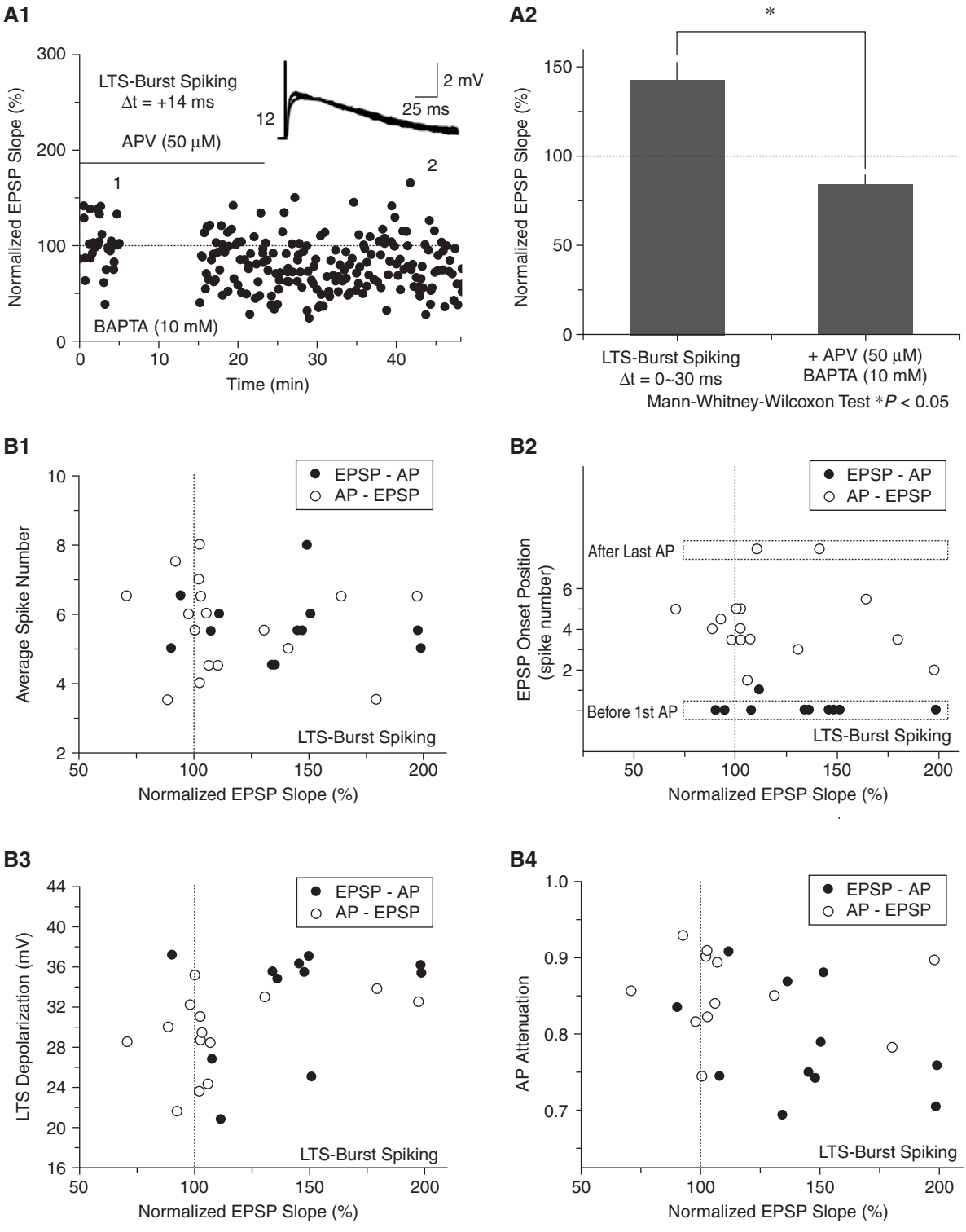

Fig. 3. The synaptic plasticity was blocked by APV and BAPTA in the internal solution. Moreover, it was independent of the average spike number of a single LTS-burst, relative timing of CT-EPSP and individual AP spikes, amplitude of LTS depolarization, and AP attenuation. *A1*, Typical example of the time course of CT-EPSP initial slope normalized with respect to the baseline (dots in A1) of the experiments in which LTP induced in positive-pairing condition was blocked in the presence of APV and BAPTA. The inset traces are the responses averaged over 10 sweeps of recording during baseline ("1") and 30 min after pairing ("2"). A2, Summary of the experiments in Fig. 2A and 3A1. *B*, The failure of plasticity induction by negative pairing (Fig. 2B) was not related to the average spike number (B1), the temporal relationships of CT-EPSP and individual APs (B2), the amplitude of depolarization mediated by LTS (B3) and the AP attenuation (B4) within LTS-burst spiking during the pairing process. "EPSP-AP" and "AP-EPSP" correspond to the pairing conditions of $\Delta t > 0$ and $\Delta t < 0$, respectively.

current injection (also at ~40 ms following the 1st AP) was measured. AP attenuation (Fig. 3, B4) was calculated as the ratio of the amplitude of the 1st AP to that of the last AP in LTS-burst spiking, both of which were measured from the membrane potential before the current injection.

All data were presented as means ± SEM. For the LTP experiments, statistical significance was assessed with nonparametric Mann-Whitney-Wilcoxon U test or Wilcoxon matched-pairs sign-ranked test. For correlation analysis, statistical significance was assessed by nonparametric Spearman's rank-order correlation test. The criterion for significance was $P < 0.05$.

Histochemistry

In all experiments, the recorded neuron was filled by passive diffusion of biocytin from the patch pipette. After recording, the brain slices were fixed with 4% paraformaldehyde in 0.1 M phosphate buffer (PB, pH 7.4) at 4°C overnight. They were rinsed with PB several times and subjected to histochemical staining procedures without further sectioning. Briefly, slices were treated with 3% H_2O_2 in PB for 30 min and then with 0.03% Triton X-100 in phosphate-buffered saline (PBST). They were incubated with 2% bovine serum albumin (BSA) and 10% normal goat serum (NGS) in PBST for 1 h at room temperature, followed by incubation with avidin-biotinylated-horseradish peroxidase complex in PBST (at a 1: 100 dilution; Vector Laboratories, Burlingame, CA, USA) at 4°C overnight. Finally, the cells were visualized using 3,3'-diaminobenzidine (DAB) as the chromogen. The staining results of the biocytin-filled neurons were examined and photographed under bright-field microscopy.

Results

Recording of CT-EPSP in TC Relay Neurons in the VBN

All the recorded neurons were located in the VBN (Fig. 1A), as confirmed by *post hoc* histochemistry for visualizing the injected biocytin. Previously described morphological and physiological criteria for identification of thalamic relay neurons were adopted (9, 10, 22, 25). Briefly, a thalamic relay neuron has a polygonal soma, 6~10 large primary dendrites with bushy appearance of arborization (Fig. 1B), and displays V_m-dependent dual firing modes (continuous and in LTS-bursts) with the watershed V_m for mode switching at ~-60 mV and a clear voltage sag upon hyperpolarizing current injection at $V_m <$ -70 mV (Fig. 1C). To evoke CT-EPSPs, a stimulating electrode was positioned locally in the VBN or *ic* to recruit CT synapses. Synaptic activity was considered as originating from the CT pathway, given that they showed linear stimulus-response relationship, paired-pulse facilitation (PPF; as shown in Fig. 1D) and conduction supernormality (9, 14, 22) (Fig. 1D).

Spike-Timing-Dependent Plasticity of CT-EPSP Induced by Pairing CT-EPSP with LTS-Burst Spiking

The burst spiking of TC relay neurons mediated by T-type voltage-gated calcium channels (T-VGCCs) was considered to be critically involved in state-dependent information relay (1, 11, 16, 20, 28, 29); however, the impact of this firing pattern on synaptic plasticity in the thalamus remained unknown. This issue is important for the understanding of thalamic information processing. To address this question, we examined the effect of pairing presynaptic stimulation with postsynaptic LTS-burst spiking (induced by somatic current injection with the V_m held at ~-70 mV) at 0.167 Hz for 100 times on CT-EPSPs. As shown in Fig. 2, this paired pre- and post-synaptic activities resulted in LTP of CT-EPSPs, given that application of presynaptic stimulation preceded that of postsynaptic spiking and the timing difference was within a window of 30 ms (Fig. 2A; LTP = 143 ± 10 % of the baseline, n = 11; $P < 0.01$). Reversing the temporal order of pre- and post-synaptic stimulations with the timing difference constrained to a window of 30 ms did not result in a long-term plastic change of CT-EPSPs to a significant level (113 ± 9% of the baseline, n = 14; $P > 0.05$) (Fig. 2B).

The spike-timing-dependent LTP was blocked by the addition of an NMDA receptor (NMDAR) antagonist, APV (50 μM), into the bath medium combined with a calcium chelator, BAPTA (10 mM), in the internal solution (Fig. 3A) (Δt = 0~30 ms: LTP = 84 ± 5% of the baseline, n = 4; $P < 0.05$ compared with the control condition shown in Fig. 2A), showing that the induction of LTP was NMDAR-dependent. Taken together, the above results showed that the induction of LTP at CT synapses depended on the timing and temporal order of correlated pre- and post-synaptic activities, and the activation of NMDAR.

Carefully viewing the data, we noticed there were trial-to-trial variabilities of LTS-burst spiking, including the spike number (the range of average AP number: 3.5~8) and the timing of burst spiking. The variability may be attributable to intrinsic variability of neuronal properties, such as the biophysical states of active conductances, which can result in the variability of pairing conditions (*i.e.*, variability in the total AP number and temporal relationship of CT-EPSP and individual APs during the pairing). In order to examine if such kinds of variability obscured the relation between Δt and synaptic plasticity, we further tested the correlation between these factors

and synaptic plasticity. The results showed that the plasticity was correlated neither to the average spike number of LTS-burst spiking (Fig. 3, B1, $P > 0.05$ for $\Delta t > 0$ and $\Delta t < 0$, separately or together) nor to the timing of individual APs in terms of (average) EPSP onset position with respect to AP spike number (Fig. 3, B2, $P > 0.05$ for $\Delta t > 0$ and $\Delta t < 0$, separately or together), suggesting that failure of plasticity induction by negative pairing could not be accounted for by the confounding effect of the variability.

It has been shown that spike-timing-dependent LTP is correlated with the amplitude of postsynaptic depolarization (31). Our results are consistent with this observation: within a comparable time window, LTP could be induced by pairing CT-EPSP *with* burst AP spiking underlain by LTS (Fig. 2A; LTS depolarization: 32.8 ± 1.7 mV); on the contrary, no significant LTP could be induced by pairing CT-EPSP with high-frequency spiking which mimics the AP spiking of an LTS-burst *without* the underlying LTS (see Fig. 4A below; residual depolarization following high-frequency spiking: 6.1 ± 0.6 mV). A closer examination revealed that intrinsic variability of LTS depolarization and AP attenuation within an LTS-burst spiking existed, which were inversely correlated with each other (LTS depolarization *vs.* AP attenuation, $P < 0.001$); nevertheless, this variability did not confound the results of synaptic plasticity, either, since neither of them was correlated with plasticity (Fig. 3, B3 and B4; $P > 0.05$ for $\Delta t > 0$ and $\Delta t < 0$, separately or together). Taken together, these analyses showed that despite the existence of the variability of LTS-burst spiking, it did not confound the results of synaptic plasticity. Furthermore, any single factors discussed above could not account for the failure of plasticity induction in the negative-pairing experiments (Fig. 2B), supporting that the induction of spike-timing-dependent LTP at CT synapses was critically dependent on the timing of correlated pre- and post-synaptic activities.

Spike-Timing-Dependent LTP of CT-EPSP Is Dependent on LTS

Is the high-frequency spiking of APs alone sufficient to induce the LTP of CT-EPSP? Alternatively, low-threshold calcium spike might be necessary for the induction. To investigate the role of LTS in the induction of spike-timing-dependent LTP at CT synapses, we sought pharmacological agents to specifically block T-VGCCs, the channels well-established to underlie the initiation of LTS (10, 11, 29, 36). However, we found that neither nickel (Ni^{2+}) nor mibefradil blocked LTS at a low micromolar concentration at which selective blockade of T-VGCCs was ensured (data not shown). Therefore, we adopted an alternative approach by pairing CT-EPSP with high-frequency spiking, which was induced by five brief somatic current injections at 125 Hz (the average number and frequency of AP spiking of a typical LTS-burst) with the V_m held at ~-55 mV, at 0.167 Hz for 100 times (see Materials and Methods; Fig. 4, A2 and B2). In this way, the high-frequency spiking mimics the AP spiking but lacks the underlying LTS of an LTS-burst. In contrast to the case of pairing CT-EPSP with LTS-burst spiking, we found that synaptic plasticity could be induced neither by positive (Δt = 0~50 ms: 121 ± 23% of the baseline, n = 6; $P > 0.05$) nor by negative pairing (Δt = 0~-55 ms: 112 ± 19% of the baseline, n = 4; $P > 0.05$) (Fig. 4). Our results indicate that, for the induction of spike-timing-dependent LTP of CT-EPSP, burst spiking of APs is not sufficient, and the involvement of low-threshold calcium spike during the pairing process is required.

Discussion

In this study, we reported that pairing CT-EPSP with postsynaptic spiking induced a spike-timing-dependent LTP at CT synapses on thalamic relay neurons. In particular, we for the first time demonstrated that induction of this LTP critically depended on the specific pattern of postsynaptic spiking: the LTP was induced by pairing AP burst spiking driven by LTS, but not by pairing ordinary high-frequency APs alone. Its induction was dependent on spike timing, and could be blocked pharmacologically. Our novel finding is the first experimental account which directly addresses the role of low-threshold calcium spike in induction of LTP in thalamus.

Previous studies have suggested that backpropagation of AP into dendrites provides postsynaptic depolarization and contributes to induction of synaptic plasticity (2, 18, 34). Moreover, it has been shown that the frequency of postsynaptic spiking is a critical factor for induction of LTP (18, 19, 30). It could be that a high spiking frequency can enhance the backpropagation of APs (16, 32) and support their temporal summation better than a low spiking frequency, thereby providing more postsynaptic depolarization to facilitate NMDAR activation and LTP induction. Although the LTP induction at CT synapses also depended on NMDAR activation, it appears that high-frequency spiking is not sufficient: the pairing of postsynaptic spiking of thalamic neurons induced by brief somatic current injections at 125 Hz with the V_m held at ~-55 mV failed to induce LTP. This spiking pattern, including the AP number (five) and the high frequency (125 Hz), was comparable to that of natural LTS-burst spiking (elicited with the V_m held at ~-70 mV) with the only difference being the holding V_m and, therefore, the availability of low-threshold

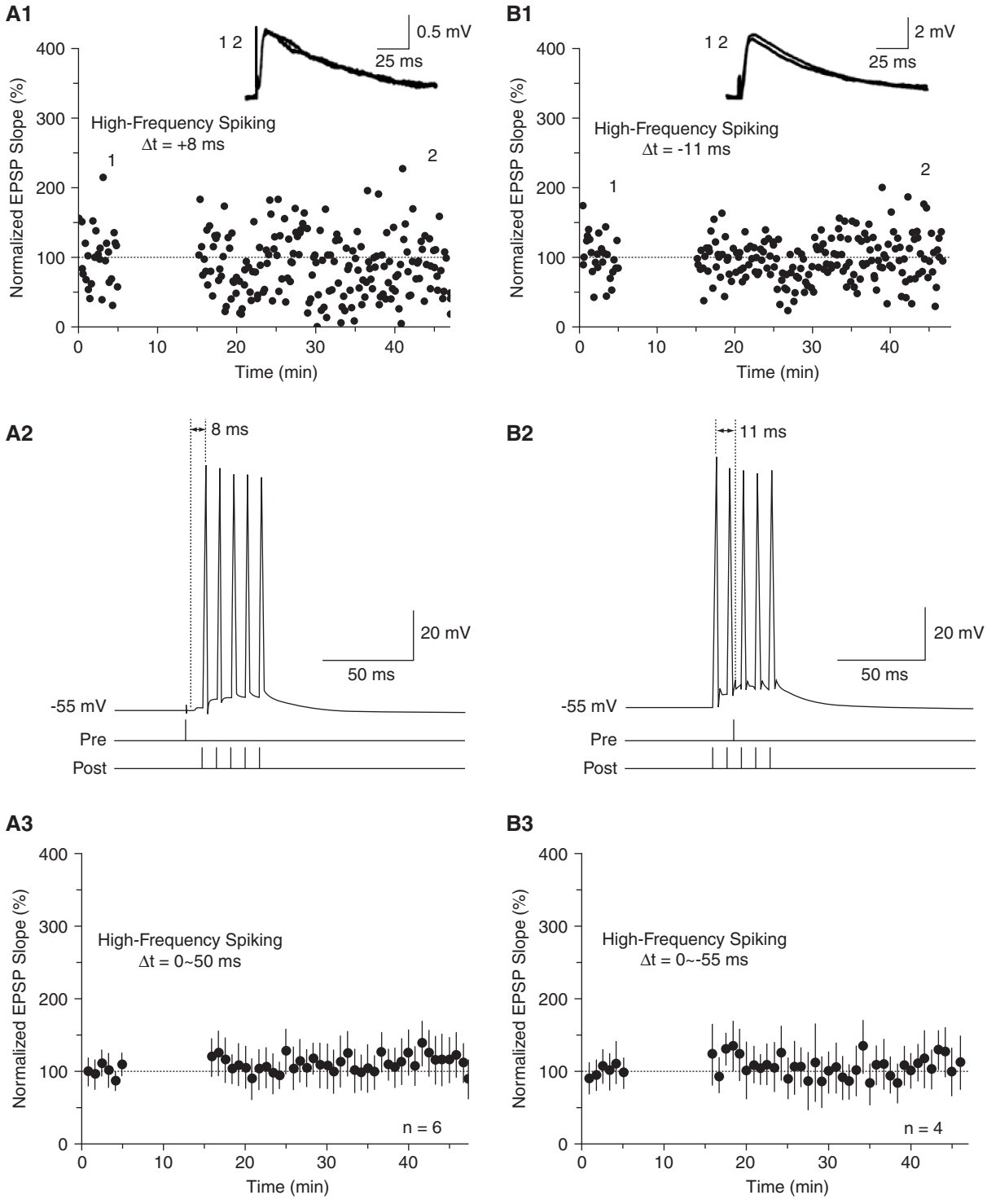

Fig. 4. Pairing CT-EPSP with high-frequency spiking, which mimics the AP spiking but lacks the underlying LTS of a single LTS-burst, could not induce synaptic plasticity of CT-EPSP. *A*, Typical example of the time course of CT-EPSP initial slope normalized with respect to the baseline (dots in A1), representative voltage trace during the pairing (A2), and summarized time course (A3) of the experiments in which CT-EPSP was paired with high-frequency spiking at positive intervals (0~50 ms). *B*, Typical example of the time course of normalized CT-EPSP initial slope (dots in B1), representative voltage trace during the pairing (B2), and summarized time course (B3) of the experiments in which CT-EPSP was paired with high-frequency spiking at negative intervals (0~-55 ms). The inset traces in A1 and B1 are the responses averaged over 10 sweeps of recording during baseline ("1") and 30 min after pairing ("2"). The line drawings at the bottom of A2 and B2 indicate the timing of extracellular stimulation ("Pre"; 580 μA, 50 μs in A2 and 30 μA, 50 μs in B2) and somatic current injections ("Post"; 1.7 nA, 1 ms in A2 and 1.1 nA, 1 ms in B2; both at 125 Hz), which were paired at 0.167 Hz for 100 times. Note that the V_m during pairing was held at ~-55 mV.

calcium spike, which can account for the significant difference of the postsynaptic depolarization following APs between LTS-burst spiking (Fig. 2, A2) and high-frequency spiking induced by somatic current injections (Fig. 4, A2). For the above reasons, we argue that while the high-frequency backpropagating APs alone are not sufficient, low-threshold calcium spike is a critical factor for the LTP induction at CT synapses.

Depolarization of membrane potential to -55 mV may induce several changes in intrinsic membrane properties of neurons. Since $GABA_A$ receptors and glycine receptors were blocked, the lack of LTP cannot be explained by an increase of chloride driving force and the accompanying inhibitory drives onto postsynaptic neurons during the depolarized pairing condition. Sensitive to this level of depolarization, T-VGCCs, hyperpolarization-activated nonselective cationic channels (h-channels) and A-type potassium channels are candidate voltage-dependent conductances which could be involved in the induction process. Considering channel biophysics, however, depolarization deactivates h-channels, which makes dendrites less leaky (7), and inactivates A-type potassium channels, which facilitates dendritic excitability (8), it is less likely that change of these conductances was responsible for the lack of LTP. T-VGCCs are well established in their subthreshold voltage dependence and the role in mediating low-threshold calcium spike of thalamic neurons (9-11, 30, 36), and we, therefore, speculate potential involvement of T-VGCCs in the induction of LTP.

In thalamic relay neurons, direct patch-clamp recording, calcium imaging, computer modeling and immunocytochemistry studies have indicated that T-VGCCs are expressed throughout the dendritic arbor, especially concentrated at proximal dendritic compartments (5, 21, 23, 24, 35, 36), and are critical for generating and shaping the LTS response (5). During the pairing condition of LTS-burst spiking, it is possible that the amplitude and duration of back-propagating APs are enhanced by these dendritic T-VGCCs on their arrival at activated synapses (15, 18, 32), thereby facilitating LTP induction. Another possibility for T-VGCCs to enhance spike-timing-dependent LTP could be that additional calcium influx flows into the postsynaptic neuron, which in turn activates calcium-dependent signaling pathways required for LTP induction at CT synapses.

In order to directly test the linkage between the activation of T-VGCCs and induction of LTP, we have carefully examined the specificity of some commonly-used T-VGCC blockers, including nickel (Ni^{2+}) and mibefradil, in our experimental system. Unfortunately, it was found that neither of them could selectively block T-VGCCs (9). If specific T-type channel blockers prevented LTP induction, it would be very helpful to clarify the relationship between LTP and T-type channel activation, which, however, cannot be achieved due to the lack of a selective pharmacological tool. Therefore, we would rather emphasize at this point that our speculation over the role of T-VGCCs aims to provide a hypothetical mechanism underlying the induction of LTP, and further experiments need to be done carefully to elucidate the molecular mechanisms of LTP at CT synapses.

Considering the dendritic origin of low-threshold calcium spike in relay neurons, where a variety of sensory and modulatory inputs make contacts (11, 12, 17, 29, 31), the novel role of calcium spike in LTP induction found in this study might implicate new physiological regulation on synaptic plasticity of CT pathway. For example, medial lemniscal synapses convey powerful sensory input onto proximal dendritic compartments of VBN relay neurons, which could exert significant influences over the generation of dendritic calcium spike and, thus, the induction of synaptic plasticity at CT synapses.

In conclusion, CT synapses on thalamic relay neurons in the VBN can express spike-timing-dependent LTP, and the activation of low-threshold calcium spike appeared to be crucial for induction of this form of LTP. Taking our present and previous findings (9) together, it seems that CT synaptic input could undergo long-lasting, bi-directional plastic change in their efficacy in a spiking-state-dependent manner. Wolfart and colleagues (35) have shown that transfer function of thalamic relay neurons can be modulated by background synaptic noise mostly originating from the CT pathway. As a consequence, we suggest that the spiking-state-dependent plasticity of CT synapses may respond to various physiologically relevant variables and dynamically fine-tune thalamocortical information relay accordingly.

Acknowledgments

The text of this section should be: “This work was supported by a grant from the National Science Council, Taiwan (NSC100-2311-B-002-003-MY3).”

References

1. Bal, T. and McCormick, D.A. Mechanisms of oscillatory activity in guinea-pig nucleus reticularis thalami *in vitro*: a mammalian pacemaker. *J. Physiol.* 468: 669-691, 1993.
2. Dan, Y. and Poo, M.M. Spike timing-dependent plasticity of neural circuits. *Neuron* 44: 23-30, 2004.
3. Deschênes, M., Veinante, P. and Zhang, Z.W. The organization of corticothalamic projections: reciprocity versus parity. *Brain Res. Rev.* 28: 286-308, 1998.
4. Destexhe, A. Modelling corticothalamic feedback and the gating of the thalamus by the cerebral cortex. *J. Pysiol. (Paris)* 94: 391-410, 2000.

5. Destexhe, A., Neubig, M., Ulrich, D. and Huguenard, J. Dendritic low-threshold calcium currents in thalamic relay cells. *J. Neurosci*. 18: 3574-3588, 1998.
6. Ergenzinger, E.R., Glasier, M.M., Hahm, J.O. and Pons, T.P. Cortically induced thalamic plasticity in the primate somatosensory system. *Nat. Neurosci*. 1: 226-229, 1998.
7. George, M.S., Abbott, L.F. and Siegelbaum, S.A. HCN hyperpolarization-activated cation channels inhibit subthreshold EPSPs through interactions with M-Type K^+ channels. *Nat. Neurosci*. 12: 577-584, 2009.
8. Hoffman D.A., Magee, J.C., Colbert, C.M. and Johnston, D. K^+ channel regulation of signal propagation in dendrites of hippocampal pyramidal neurons. *Nature* 387: 869-875, 1997.
9. Hsu, C.L., Yang, H.W., Yen, C.T. and Min, M.Y. Comparison of synaptic transmission and plasticity between sensory and cortical synapses on relay neurons in the ventrobasal nucleus of the rat thalamus. *J. Physiol*. 588: 4347-4363, 2010.
10. Jahnsen, H. and Llinás, R. Electrophysiological properties of guinea-pig thalamic neurones: an *in vitro* study. *J. Physiol*. 349: 205-226, 1984.
11. Jones, E.G. The thalamus. Cambridge, Cambridge University Press, 2007.
12. Killackey, H.P. and Sherman, S.M. Corticothalamic projections from the rat primary somatosensory cortex. *J. Neurosci*. 23: 7381-7384, 2003.
13. Krupa, D.J., Ghazanfar, A.A. and Nicolelis, M.A. Immediate thalamic sensory plasticity depends on corticothalamic feedback. *Proc. Natl. Acad. Sci. USA* 96: 8200-8205, 1999.
14. Landisman, C.E. and Connors, B.W. VPM and PoM nuclei of the rat somatosensory thalamus: intrinsic neuronal properties and corticothalamic feedback. *Cereb. Cortex* 17: 2853-2865, 2007.
15. Le Masson, G., Renaus-Le Masson, S., Debay, D. and Bal, T. Feedback inhibition controls spike transfer in hybrid thalamic circuit. *Nature* 417: 854-858, 2002.
16. Lisman, J. and Spruston, N. Postsynaptic depolarization requirements for LTP and LTD: a critique of spike timing-dependent plasticity. *Nat. Neurosci*. 8: 839-841, 2005.
17. Liu, X.B., Honda, C.N. and Jones, E.G. Distribution of four types of synapse on physiologically identified relay neurons in the ventral posterior thalamic nucleus of the cat. *J. Comp. Neurol*. 352: 69-91, 1995.
18. Magee, J.C. and Johnston, D. A synaptically controlled, associative signal for Hebbian plasticity in hippocampal neurons. *Science* 275: 209-213, 1997.
19. Markram, H., Lübke, J., Frotscher, M. and Sakmann, B. Regulation of synaptic efficacy by coincidence of postsynaptic APs and EPSPs. *Science* 275: 213-215, 1997.
20. McCormick, D.A. and Feeser, H.R. Functional implications of burst firing and single spike activity in lateral geniculate relay neurons. *Neuroscience* 39: 103-113, 1990.
21. Mckay, B.E., McRory, J.E., Molineux, M.L., Hamid, J., Snutch, T.P., Zamponi, G.W. and Turner, R.W. Ca_v3 T-type calcium channel isoforms differentially distribute to somatic and dendritic compartments in rat central neurons. *Eur. J. Neurosci*. 24: 2581-2594, 2006.
22. Miyata, M. and Imoto, K. Different composition of glutamate receptors in corticothalamic and lemniscal synaptic responses and their roles in the firing responses of ventrobasal thalamic neurons in juvenile mice. *J. Physiol*. 575: 161-174, 2006.
23. Munsch, T., Budde, T. and Pape, H.C. Voltage-activated intracellular calcium transients in thalamic relay cells and interneurons. *Neuroreport* 8: 2411-2418, 1997.
24. Murphy, P.C. and Sillito, A.M. Corticofugal feedback influences the generation of length tuning in the visual pathway. *Nature* 329: 727-729, 1987.
25. Peschanski, M., Lee, C.L. and Ralston, H.J. The structural organization of the ventrobasal complex of the rat as revealed by the analysis of physiologically characterized neurons injected intracellularly with horseradish peroxidase. *Brain Res*. 297: 63-74, 1984.
26. Reichova, I. and Sherman, S.M. Somatosensory corticothalamic projections: distinguishing drivers from modulators. *J. Neurophysiol*. 92: 2185-2197, 2004.
27. Rouiller, E.M. and Welker, E. A comparative analysis of the morphology of corticothalamic projections in mammals. *Brain Res. Bull*. 53: 727-741, 2000.
28. Sherman, S.M. Tonic and burst firing: dual modes of thalamocortical relay. *Trends Neurosci*. 24: 122-126, 2010.
29. Sherman, S.M. Thalamic relays and cortical functioning. *Prog. Brain Res*. 149: 107-126, 2005.
30. Sjöström, P.J., Turrigiano, G.G. and Nelson, S.B. Rate, timing, and cooperativity jointly determine cortical synaptic plasticity. *Neuron* 32: 1149-1164, 2001.
31. Špacek, J. and Lieberman, A.R. Ultrastructure and three-dimensional organization of synaptic glomeruli in rat somatosensory thalamus. *J. Anat*. 117: 487-516, 1974.
32. Stuart, G.J. and Häusser, M. Dendritic coincidence detection of EPSPs and action potentials. *Nat. Neurosci*. 4: 63-71, 2001.
33. Van Horn, S.C. and Sherman, S.M. Differences in projection patterns between large and small corticothalamic terminals. *J. Comp. Neurol*. 475: 406-415, 2004.
34. Williams, S.R. and Stuart, G.J. Action potential backpropagation and somato-dendritic distribution of ion channels in thalamocortical neurons. *J. Neurosci*. 20: 1307-1317, 2000.
35. Wolfart, J., Debay, D., Le Masson, G., Destexhe, A. and Bal, T. Synaptic background activity controls spike transfer from thalamus to cortex. *Nat. Neurosci*. 8: 1760-1767, 2005.
36. Zhou, Q., Godwin, D.W., O'Malley, D.M. and Adams, P.R. Visualization of calcium influx through channels that shape the burst and tonic firing modes of thalamic relay neurons. *J. Neurophysiol*. 77: 2816-2825, 1997.